

# Literature-Grounded LLMs for Predicting High Ionic Conductivity Solid-State Electrolytes

Sunggi An<sup>a,\*</sup>, Kunik Jang<sup>b,\*</sup>, Junyoung Choi<sup>b</sup>, Gunwook Nam<sup>b</sup>, Jang Wook Choi<sup>b,c</sup>, Yousung Jung<sup>b,d,e,\*</sup>

<sup>a</sup>Equal contribution <sup>a</sup>Department of Chemical and Biomolecular Engineering, Korea Advanced Institute of Science and Technology (KAIST), 291, Daehak-ro, Yuseong-gu, Daejeon 34141, South Korea <sup>b</sup>Department of Chemical and Biological Engineering, and Institute of Chemical Processes, Seoul National University, 1 Gwanak-ro, Gwanak-gu, Seoul 08826, South Korea <sup>c</sup>Seoul National University Energy Initiative (SNU EI), Seoul National University, 1 Gwanak-ro, Gwanak-gu, Seoul 08826, South Korea <sup>d</sup>Institute of Chemical Processes, Seoul National University, 1 Gwanak-ro, Gwanak-gu, Seoul 08826, South Korea <sup>e</sup>Institute of Engineering Research, Seoul National University, 1 Gwanak-ro, Gwanak-gu, Seoul 08826, South Korea

Correspondence to: Yousung Jung [yousung.jung@snu.ac.kr](mailto:yousung.jung@snu.ac.kr)

## 1. Introduction

All-solid-state batteries (ASSBs) require solid electrolytes (SEs) that deliver both high room-temperature Li<sup>+</sup> conductivity and robust stability.[1] However, discovering such materials remains challenging and slow. This is largely because ionic conductivity is governed by both composition and crystal structure, while high-quality, experimentally labeled datasets that capture these factors are still scarce.

Recent large language models (LLMs) provide a practical opportunity to incorporate literature-grounded structural descriptions (even when CIF-quality labels are scarce) into property prediction.[2,3] Herein, we present a fine-tuned, literature-grounded LLM for ionic conductivity prediction and integrate it with high-

throughput virtual screening (HTVS) and machine-learned interatomic potentials (MLIP)-based MD validation to identify promising SE candidates from Materials Project (MP) (Figure 1).

## 2. Methods

Literature dataset construction:

We curated 874 experimental entries from two prior papers,[4,5] linking compositions/ICSD IDs to source papers and extracting structure-related text from full articles.

Structural text descriptors:

We extracted structural information and categorized (basic crystal descriptors; cell/coordination; experimental notes) the Structural description from the literature to test which

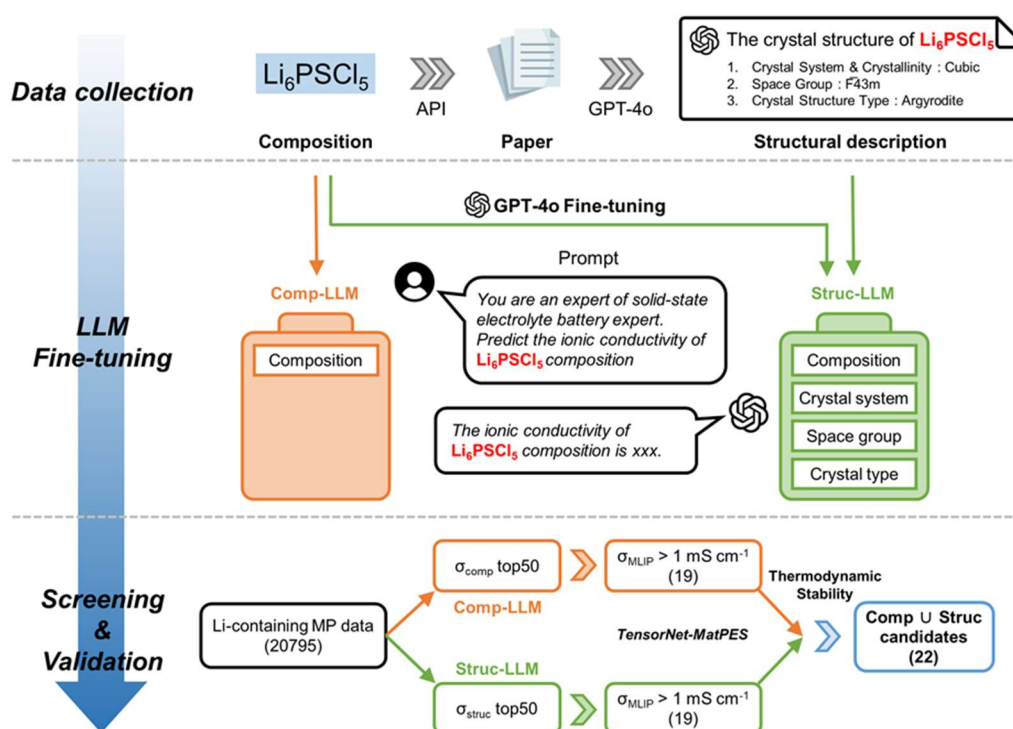


**Figure 1.** Schematic overview of this work, from data collection and model training to HTVS.

granularity best supports conductivity prediction.

LLM fine-tuning and screening pipeline:  
We fine-tuned a pretrained GPT-4o to predict log ionic conductivity, comparing Comp-LLM (composition-only) vs. Struc-LLM (composition + structural descriptors), using an 8:1:1 split and 5-fold ensembles; MP candidates were converted to text using RoboCrystallographer.[6]

Ionic conductivity validation via MLIP calculation:

Top candidates were validated by solid-state MD using TensorNet-MatPES,[7] and down-selected using MLIP calculated conductivity.

### 3. Results and Discussion

#### Regression performance and the role of structural descriptors

Both Comp-LLM and Struc-LLM exceeded a graph-based ML baseline.[8] Adding structure improved generalization with ensemble MAE and  $R^2$  of 0.704 and 0.721 for Comp-LLM and 0.689 and 0.744 for Struc-LLM. Basic crystal descriptors delivered the most reliable gains, whereas detailed cell and coordination or heterogeneous experimental narratives reduced accuracy, suggesting that noisy text can obscure transport signals.

#### HTVS results from Materials Project candidates

Applying the models to 20,795 Li-containing Materials Project entries[9], we selected the top 50 for each model and obtained 70 unique candidates after removing duplication (**Figure 2**). All exceeded the practical threshold of 0.1 mS/cm in predicted conductivity, indicating broad SE potential and enabling screening without standardized structure labels.

#### MLIP based MD validation of ranked candidates

Solid-state MD using TensorNet-MatPES[7], refined the candidate set and showed that LLM-ranked groups generally tracked MLIP-calculated conductivity trends. Prior benchmarking reported strong MLIP to AIMD correlation near  $R^2$  0.80, supporting MLIP MD as a scalable validation stage and revealing overestimation versus experimental conductivities in checks.

#### Complementarity of two LLM views and final candidates

Struc-LLM selected higher-conductivity candidates on average and the overlap between models performed best. Mean MLIP conductivities were 1.44 for Comp-LLM, 1.68 for Struc-LLM, and 1.77 mS cm<sup>-1</sup> for the overlap. Applying conductivity and stability criteria yielded 22 final candidates meeting MLIP and  $E_{\text{hull}}$  thresholds.

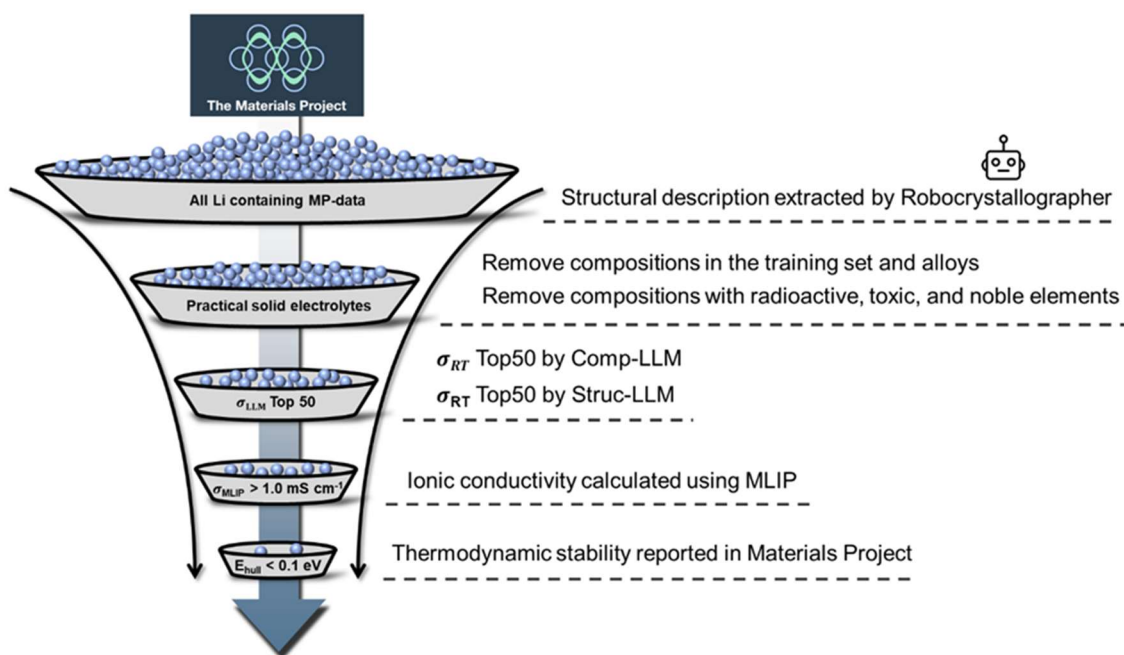


**Figure 2.** High-throughput virtual screening (HTVS) procedure for sampling promising solid electrolytes (SEs).

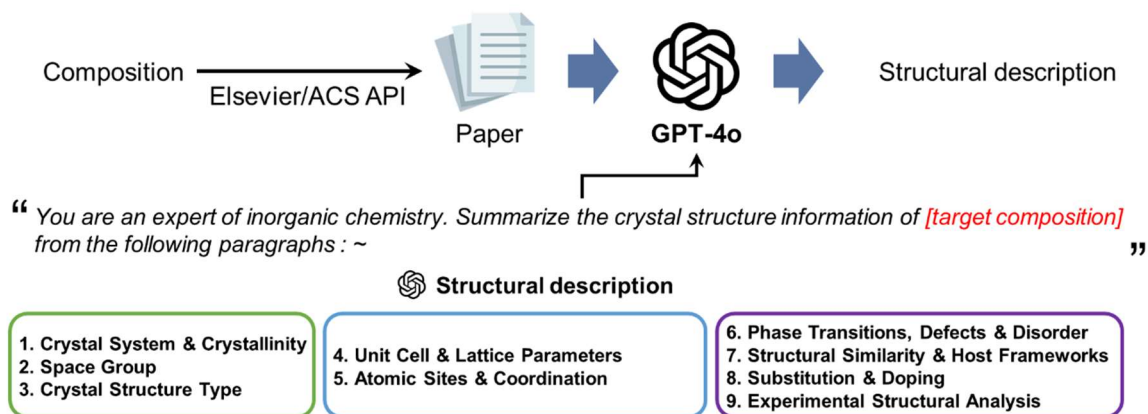
## References

- [1] Janek, J.; Zeier, W. G. Challenges in speeding up solid-state battery development. *Nature Energy* 2023, 8 (3), 230-240, DOI: 10.1038/s41560-023-01208-9
- [2] Zhang, Q.; Ding, K.; Lv, T.; Wang, X.; Yin, Q.; Zhang, Y.; Yu, J.; Wang, Y.; Li, X.; Xiang, Z. Scientific large language models: A survey on biological & chemical domains. *ACM Comput. Surv.* 2025, 57 (6), 1-38, DOI: 10.1145/3715318
- [3] Abir, A. R.; Toki Tahmid, M.; Bayzid, M. S. BioLLMNet: enhancing RNA-interaction prediction with a specialized cross-LLM transformation network. *Brief. Bioinform.* 2025, 26 (5), bbaf549, DOI: 10.1093/bib/bbaf549
- [4] Laskowski, F. A.; McHaffie, D. B.; See, K. A. Identification of potential solid-state Li-ion conductors with semi-supervised learning. *Energy Environ. Sci.* 2023, 16 (3), 1264-1276, DOI: 10.1039/d2ee03499a
- [5] Hargreaves, C. J.; Gaultois, M. W.; Daniels, L. M. A database of experimentally measured lithium solid electrolyte conductivities evaluated with machine learning. *npj Computational Mater.* 9. 2023, DOI: 10.1038/s41524-022-00951-z
- [6] Ganose, A. M.; Jain, A. Robocrystallographer: automated crystal structure text descriptions and analysis. *MRS Communications* 2019, 9 (3), 874-881, DOI: 10.1557/mrc.2019.94
- [7] Kaplan, A. D.; Liu, R.; Qi, J.; Ko, T. W.; Deng, B.; Riebesell, J.; Ceder, G.; Persson, K. A.; Ong, S. P. A foundational potential energy surface dataset for materials. *arXiv preprint arXiv:2503.04070* 2025, DOI: 10.48550/arXiv.2503.04070
- [8] Wang, S.; Gong, S.; Böger, T.; Newnham, J. A.; Vivona, D.; Sokseiha, M.; Gordiz, K.; Aggarwal, A.; Zhu, T.; Zeier, W. G. Multimodal Machine Learning for Materials Science: Discovery of Novel Li-Ion Solid Electrolytes. *Chem. Mater.* 2024, 36 (23), 11541-11550, DOI: 10.1021/acs.chemmater.4c02257
- [9] Horton, M. K.; Huck, P.; Yang, R. X.; Munro, J. M.; Dwaraknath, S.; Ganose, A. M.; Kingsbury, R. S.; Wen, M.; Shen, J. X.; Mathis, T. S. Accelerated data-driven materials science with the Materials Project. *Nat. Mater.* 2025, 24 (10), 1-11, DOI: 10.1038/s41563-025-02272-0

## Appendix A. Extraction process of structural description from the bibliographic information using LLM.

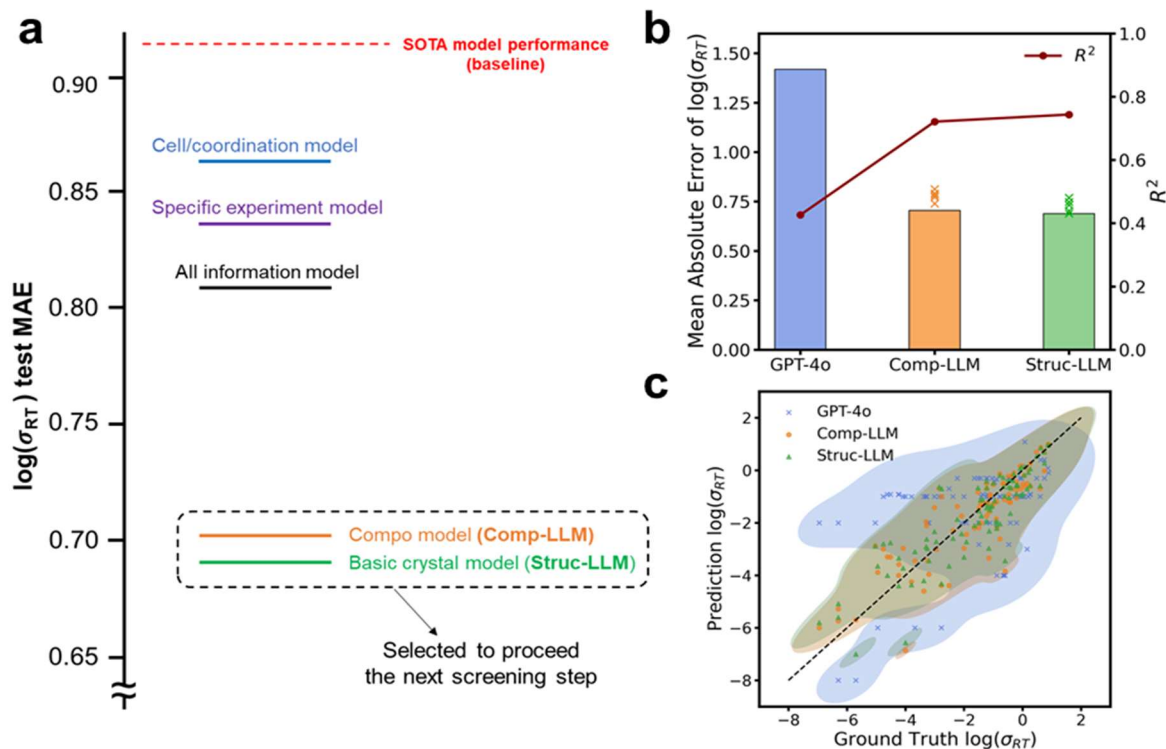
3 Categories of 9 structural descriptions are described in three boxes. The green box includes basic information, the blue box includes structural information, and the purple box includes experimental information.

### Structure Description Extraction using LLM

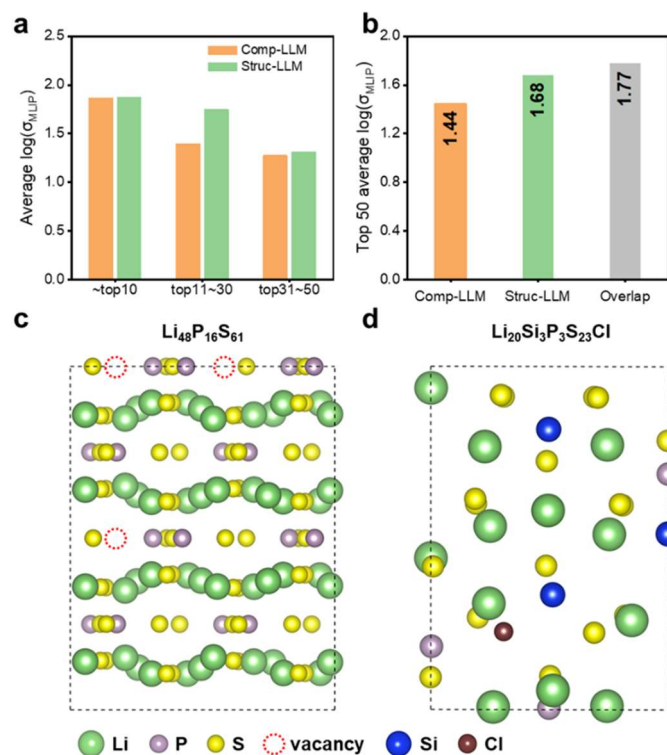


## Appendix B. Performance of our prediction model.

(a) Performance comparison between prior work and each categorized information involved models. (b) Performance of ensemble prediction of Comp-LLM and Struc-LLM between non-finetuned predictions. (c) Parity plots of each prediction, the dashed line is the  $y=x$  line.



## Appendix C. The result of HTVS.



(a) Average  $\log(\sigma_{MLIP})$  values of the top 10, 11-30, and 31-50 entries for each model. (b) Average  $\log(\sigma_{MLIP})$  values of the top 50 entries for each model and overlapped data. Representative structures of the final candidate materials: (c)  $Li_{48}P_{16}S_{61}$  (mp-1001069), (d)  $Li_{20}Si_3P_3S_{23}Cl$  (mp-1097035).